JOURNAL OF FORENSIC SCIENCES

J Forensic Sci, 2012
doi: 10.1111/j.1556-4029.2012.02298.x
Available online at: onlinelibrary.wiley.com

PAPER

ENGINEERING SCIENCES

Scott R. Lucas,[1] *Ph.D., P.E.; Joseph C. McGowan,*[2] *Ph.D., P.E.; Tack C. Lam,*[3] *M.D., Ph.D.; Gary T. Yamaguchi,*[4] *Ph.D., P.E.; Matthew Carver,*[5] *B.S.; and Andrew Hinz,*[5] *B.S.*

Assessment of the TASER XREP Blunt Impact and Penetration Injury Potential Using Cadaveric Testing*,†

ABSTRACT: TASER International's extended range electronic projectile (XREP) is intended to be fired from a shotgun, impact a threat, and apply remote neuromuscular incapacitation. This study investigated the corresponding potential of blunt impact injury and penetration. Forty-three XREP rounds were deployed onto two male human cadaver torsos at impact velocities between 70.6 and 95.9 m/sec (232 and 315 ft/sec). In 42 of the 43 shots fired, the XREP did not penetrate the abdominal wall, resulting in superficial wounds only. On one shot, the XREP's nose section separated prematurely in flight, resulting in penetration. No bony fractures were observed with any of the shots. The viscous criterion (VC), blunt criterion (BC), and energy density (*E/A*) were calculated (all nonpenetrating tests, average ± 1 standard deviation: VC: 1.14 ± 0.94 m/sec, BC: 0.77 ± 0.15, *E/A*: 22.6 ± 4.15 J/cm^2) and, despite the lack of injuries, were generally found to be greater than published tolerance values.

KEYWORDS: forensic science, TASER XREP, cadaver, blunt impact trauma, penetration, injury risk, biomechanics

Historically, nonlethal munitions such as bean bag rounds and rubber "rockets" have been utilized by firing them from a shotgun or other firearm. Alternatively, stun guns are used which are typically deployed at short range relative to the nonlethal munitions. TASER International recently designed a new nonlethal munition that combines the principles of the traditional nonlethal munitions with the technology of stun guns. This hybrid design was coined the extended range electronic projectile (XREP). The TASER XREP is designed as a wireless electronic control device capable of being deployed from a 12-gauge pump action shotgun out to a range of *c.* 30.5 m (100 ft). Upon contact with the target, the XREP delivers neuromuscular incapacitation (NMI) effect for 20 sec. Owing to the wireless nature of the TASER XREP, it now affords the user an opportunity to engage multiple suspects, which serves as a force multiplier for the individual officer. The sustained NMI effect allows adequate time for the user to approach and detain the threat. We investigated the potential of a blunt and/or penetration injury from an XREP impact. This paper presents the results of that evaluation.

Regarding blunt impact, several variables are reported in the biomechanics literature as injury metrics including peak force, peak or impact velocity, and chest compression. In this paper, the two criteria for evaluating blunt impact injury potential from nonlethal munitions are the viscous criterion (VC) and the blunt criterion (BC). The VC_{max} introduced by Lau and Viano (1) is the maximum instantaneous product of the velocity and chest compression:

$$VC_{max} = \max[v(t) \cdot C(t)] \quad (1)$$

where $v(t)$ is the instantaneous velocity and $C(t)$ is the instantaneous chest compression, where chest compression is defined as a ratio of depth of the thorax compression because of blunt impact to the initial thorax depth. As stated by Lau and Viano (1), "crushing injuries" result from low rates of deformation (*c.* 1–2 m/sec), "viscous injuries" result from moderate rates of deformation (2–20 m/sec), and "blast injuries" result from rates beyond *c.* 30–40 m/sec. VC_{max} was introduced in the automotive industry, and the majority of the biomechanics literature evaluating VC_{max} pertains to automobile impact rates simulating scenarios such as impact between the thorax and the steering wheel or airbag.

The BC has been historically used as a munition design criterion (2,3). BC accounts for the kinetic energy of the projectile and the geometry of the torso:

$$BC = \ln\left[\frac{(1/2)mv^2}{M^{1/3}Td}\right] \quad (2)$$

where m, v, and d are the mass, velocity, and diameter of the projectile, and M and T are the total mass of the torso and the skin–muscle–fat thickness of the torso at the location of impact.

[1]ECRI Institute, 5200 Butler Pike, Plymouth Meeting, PA.
[2]Exponent, Inc., 3401 Market Street, Suite 300, Philadelphia, PA.
[3]Exponent, Inc., 5401 McConnell Avenue, Los Angeles, CA.
[4]Exponent, Inc., 23445 North 19th Avenue, Phoenix, AZ.
[5]TASER International, Inc., 17800 North 85th Street, Scottsdale, AZ.

*Presented in part at the 62nd Annual Meeting of the American Academy of Forensic Sciences, February 22–27, 2010, in Seattle, WA.
†Funded in part by TASER International and by Exponent, Inc.

Received 9 Dec. 2010; and in revised form 3 Aug. 2011; accepted 29 Oct. 2011.

Penetration potential from nonlethal munitions can be evaluated using the energy density, E/A, which accounts for the kinetic energy of the projectile, $E = (1/2)mv^2$, and the impact cross-sectional area, A. In this study, XREP penetration is defined as disruption of the peritoneum deep to skin–muscle–fat tissue layers.

Computational and physical models are useful and desired in biomechanical evaluations because of their repeatability; however, for accurate injury prediction capabilities, it is critical that these models are validated using cadaver and/or live data at the loading rates specific to the application of interest. Using these criteria, currently there exist no models suitable for the evaluation of the XREP, which is fired at *c.* 80 m/sec; therefore, a cadaveric study was undertaken to provide the foundation for such a model. This study is the first cadaveric evaluation of the current XREP design. The data are critical in the assessment of a nonpenetrating XREP firing velocity and in the development of human surrogates (test dummies) and injury criteria suitable for this application. In addition, the test results provide useful data for desired impact velocities in real-world applications.

Methods

Test Subjects

Two human cadaveric torsos were procured in accordance with Exponent's Internal Review Board. The torso donor total body specifications are listed in Table 1. The torsos were frozen postmortem, were not chemically preserved, and were completely thawed prior to testing. They were received with the head and neck, upper extremities, and lower extremities removed. Torso 2 contained the proximal humeri and femurs, while Torso 1 only contained the proximal femurs. For both specimens, the cause of death did not affect their structural properties.

Test Setup and Protocol

All tests were designed and directed by Exponent staff and within the guidance and approval of Exponent's Internal Review Board, which includes review from an external independent reviewer. The test setup consisted of an air cannon, which was provided by TASER, aimed at the target torso. The air cannon was previously calibrated to establish the relationship between the air cannon pressure and the desired muzzle velocity. The torso was placed upright on an adjustable positioning apparatus (Fig. 1). The impact location was controlled by moving the torso and positioning fixture laterally and vertically. The firing distance was established by positioning the air cannon cart assembly. High-speed video cameras were positioned orthogonally to (90°) and obliquely to (about 45°) the projectile paths, looking toward the impact locations. The test round used

TABLE 1—*Cadaver torso donor information.*

Torso Number	Specimen Number	Gender	Age	Total Body Stature (cm)*	Total Body Mass (kg)*	BMI
1	T08002R	Male	46	172.7	74.8	25
2	T08001R	Male	52	182.9	74.8	22

BMI, body mass index.
*Stature and mass were the original donor data and measured prior to removal of the head and extremities.

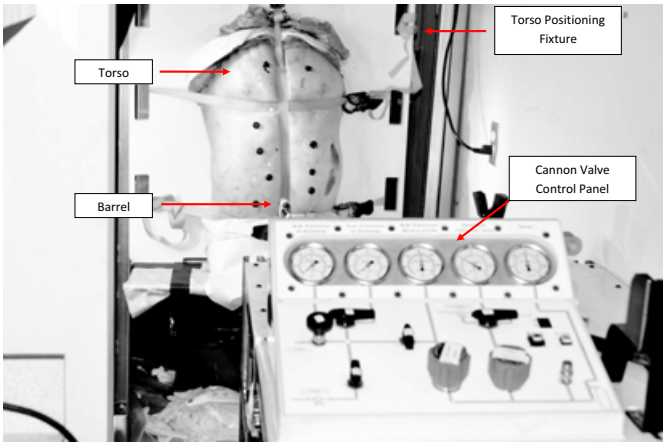

FIG. 1—*Air cannon in firing position. High-speed cameras (not shown) were located to the left of the torso. The black circles on the torso are the tip sections of fired extended range electronic projectiles.*

in this test series was the XREP manufactured and provided by TASER International (Fig. 2).

A total of 43 shots impacted the torsos, with 12 shots on the posterior aspect of Torso 1, 14 shots on the anterior aspect of Torso 1, and 17 shots on the anterior aspect of Torso 2. It was decided to not fire shots on the posterior aspect of Torso 2 after observing the results from Torso 1. The anterior torso is potentially more vulnerable to impact and penetration; thus, research efforts were focused mainly on the anterior aspect. Testing variables included impact location, firing distance, firing pressure, and barrel type. A range of air cannon firing pressures and corresponding velocities were utilized, up to the maximum capacity of the air cannon. Specifically, the tested impact velocities from the entire series ranged from 71 to 96 m/sec (230–315 ft/sec). Two tests (1A2 and 1B2) were fired at a range of 4.6 m (15 ft), and all of the other tests were fired at 0.46 m (1.5 ft). The closer distance was chosen for repeatability of the impact velocity, as the air cannon was calibrated for air pressure and firing (not impact) velocity. The two tests at the longer distance were conducted with a rifled barrel to allow the XREP to reach its steady-state rotational velocity prior to impact. The complete test matrix is provided in Table 2. Pre- and posttest photographs were taken, and high-speed video was recorded at 16,000 frames/sec for the orthogonal (side) camera and at 8000 frames/sec for the oblique camera. Each XREP was weighed after the test series was completed.

Medical Imaging and Posttest Internal Examinations

The torsos were examined with magnetic resonance imaging (MRI) and computed tomography (CT) before and after the XREP firing experiments. CT scanning was carried out on a GE Lightspeed Ultra (GE Medical Systems, Waukesha, WI) running LightSpeedApps 308I.2_H3.1MS. For the MRI scans, a Siemens Trio scanner running Syngo MR A30 4VA30A (Malvern, PA) was used to provide imaging at 3.0 T. Body coil transmission and reception was used. The imaging protocol included both spin and gradient echo images in the axial and coronal planes. For the posttest MR images, MPRage and T1 SE sequences were performed.

The torsos were internally examined after both the testing and posttest imaging. Before the initial dissection of the abdomen

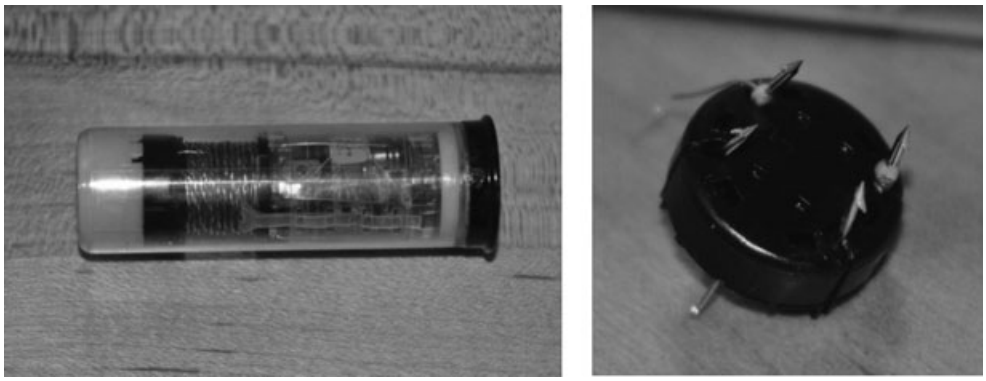

FIG. 2—*Left: Representative extended range electronic projectile inside a 12-gauge cartridge. Right: Close-up of the detachable tip section (right).*

TABLE 2—*Test matrix.*

Torso Number	Shot	Barrel	Firing Distance (m)	Anterior/Posterior	Desired Impact Location	Cannon Firing Pressure (psi)
1	A1	Smooth	0.46	Posterior	50 mm L LAT @ ~L1	210
1	B1	Smooth	0.46	Posterior	50 mm L LAT @ ~L2	220
1	C1	Smooth	0.46	Posterior	50 mm L LAT @ ~L3	230
1	D1	Smooth	0.46	Posterior	50 mm R LAT @ ~L3	240
1	E1	Smooth	0.46	Posterior	50 mm R LAT @ ~L2	250
1	F1	Smooth	0.46	Posterior	50 mm R LAT @ ~L1	260
1	G1	Smooth	0.46	Posterior	35 mm R LAT @ ~T12	270
1	H1	Smooth	0.46	Posterior	110 mm L LAT @ ~L1	300
1	J1	Smooth	0.46	Posterior	110 mm L LAT @ ~L2	330
1	K1	Smooth	0.46	Posterior	110 mm L LAT @ ~L3	360
1	L1	Smooth	0.46	Posterior	110 mm L LAT @ ~T12	360
1	M1	Smooth	0.46	Posterior	110 mm L LAT @ ~T11	380
1	N1	Smooth	0.46	Anterior	70 mm R LAT STERNUM	300
1	P1	Smooth	0.46	Anterior	75 mm L LAT @ ~XYPHOID	300
1	Q1	Smooth	0.46	Anterior	75 mm L LAT @ ~RIB 9	300
1	R1	Smooth	0.46	Anterior	50 mm INF TO LAST SHOT	300
1	S1	Smooth	0.46	Anterior	75 mm L LAT; 60 mm INF TO LAST SHOT	300
1	T1	Smooth	0.46	Anterior	70 mm L LAT; 50 mm SUP TO LAST SHOT	300
1	U1	Smooth	0.46	Anterior	70 mm L LAT; 50 mm SUP TO LAST SHOT	300
1	V1	Smooth	0.46	Anterior	70 mm L LAT; 80 mm SUP TO LAST SHOT	300
1	W1	Smooth	0.46	Anterior	75 mm L LAT; 80 mm SUP TO LAST SHOT	300
1	X1	Smooth	0.46	Anterior	75 mm L LAT; 150 mm SUP TO LAST SHOT	300
1	Y1	Rifled	0.46	Anterior	30 mm R LAT; 15 mm SUP TO LAST SHOT	300
1	Z1	Rifled	0.46	Anterior	35 mm R LAT; MID ABD	300
1	A2	Rifled	4.6	Anterior	35 mm R LAT; 80 mm INF XYPHOID	300
1	B2	Rifled	4.6	Anterior	40 mm L LAT; 60 mm INF TO LAST SHOT	300
2	A1	Smooth	0.46	Anterior	90 mm L LAT; UPPER L CHEST	300
2	B1	Smooth	0.46	Anterior	70 mm L LAT; UPPER ABD	300
2	C1	Smooth	0.46	Anterior	70 mm L LAT; 30 mm INF TO LAST SHOT	300
2	D1	Smooth	0.46	Anterior	70 mm L LAT; 55 mm INF TO LAST SHOT	300
2	E1	Smooth	0.46	Anterior	70 mm L LAT; 60 mm SUP TO LAST SHOT	300
2	F1	Smooth	0.46	Anterior	70 mm R LAT; LOWER ABD	300
2	G1	Smooth	0.46	Anterior	70 mm R LAT; 60 mm SUP TO LAST SHOT	300
2	H1	Smooth	0.46	Anterior	70 mm R LAT; 70 mm SUP TO LAST SHOT	300
2	J1	Smooth	0.46	Anterior	70 mm R LAT; 70 mm SUP TO LAST SHOT	300
2	K1	Smooth	0.46	Anterior	70 mm R LAT; UPPER R CHEST	300
2	L1	Rifled	0.46	Anterior	45 mm R LAT; UPPER CHEST	300
2	M1	Rifled	0.46	Anterior	95 mm R LAT; UPPER ABD	300
2	N1	Rifled	0.46	Anterior	115 mm L LAT; ABD	380
2	P1	Smooth	0.46	Anterior	40 mm R LAT; UPPER ABD	380
2	Q1	Smooth	0.46	Anterior	135 mm R LAT; ABD	380
2	R1	Smooth	0.46	Anterior	40 mm LAT; R CHEST	380
2	S1	Smooth	0.46	Anterior	115 mm L LAT; LOWER ABD	300

LAT, lateral relative to torso midline; L, left; R, right; ABD, abdomen; SUP, superior; INF, inferior.

was carried out, all impact points on the frontal and back sides were marked and photo-documented. An inverted "U" incision was carried out through the abdominal muscle wall to the peritoneum from the lateral iliac crest upward along the subcostal margin to the contralateral iliac crest. The abdominal wall thickness was measured, and then, the abdominal wall was reflected to determine whether there were any interior puncture marks, visible to the eye or with dye smear.

Data Analysis

The impact velocity was calculated using the high-speed videos. First, a calibration (still) shot was captured containing two photo targets set apart by a distance of 5 inches. The targets were placed along the line of the shot as determined by a laser bore sight. For each test, the number of pixels was calculated to determine the pixel/inch ratio. From the high-speed video, the XREP excursion, and chest or abdomen compression ratios [$C(t)$, see Eq. (1)], time histories were recorded using a marker tracking software (IMAGE EXPRESS; SAI, Utica, NY), which captured and followed a pixel on the trailing edge of the XREP. The excursion and compression data were filtered in accordance with the Society of Automotive Engineers (SAE) CFC 180 filter class (4–6). Instantaneous velocity, $v(t)$, was then calculated as the time derivative of chest compression.

The evaluation of injury potential included the analysis of the pre- and posttest CT and MR images and the posttest internal examination. To evaluate the appropriateness of existing injury criteria for this application and to compare to existing biomechanics literature, the VC, BC, and *E/A* were calculated for each test. The impact velocities and XREP masses and geometry were used in these calculations.

Results

The calculated impact velocities ranged from 71 to 96 m/sec (232–315 ft/sec) and are shown in Table 3. For comparable firing pressures, the smooth barrel resulted in faster impact velocities than the internally rifled barrel. There was no appreciable decrease in impact velocity between shots fired from 0.46 m (shots 1Y1 and 1Z1) and 4.6 m (shots 1A2 and 1B2) using the rifled barrel. The XREP masses ranged from 18.1 to 20 g.

Also included in Table 3 are observations regarding XREP tip separation. From the high-speed video, it was observed that 26 of the XREP tips and bodies separated at impact resulting in the XREP bodies hanging from the tips, four of the XREP tips and bodies separated prior to impact, and 13 of the XREP tips and bodies did not separate at impact. The cross-sectional area at impact was 2.69 cm^2 for all XREPs that did not have tip separation prior to impact. For the tests with tip separation prior to impact, the cross-sectional area at impact was 2.01 cm^2.

A representative posttest MR image for Torso 1 is shown in Fig. 3. There were small opacities throughout the torso, indicating minor tissue degradation; however, there was no evidence of penetration or blunt impact trauma. The pretest and posttest MR images were similar in terms of tissue degradation. On the posterior side of Torso 1, shots 1L1 and 1M1 impacted the skin surface between the 12th rib and the posterior iliac crest at the two highest velocities among the posterior shots (1L1—91.7 m/sec and 1M1—93.9 m/sec). A posttest MR image for shot 1L1 is shown in Fig. 4. There was no apparent penetration through the posterior wall or blunt impact trauma of the internal tissues for these shots.

Examination of the pre- and posttest imaging for Torso 2 also demonstrated no apparent change associated with XREP impacts, with the exception of the XREP that penetrated the torso from shot 2Q1. A posttest CT image of Torso 2 shows the XREP from shot 2Q1 at its final location inside the abdomen (Fig. 5). MR imaging of the area around the penetrated XREP (Fig. 6) was compromised because of susceptibility artifact, causing the area around the XREP to appear as a large, vacant area. For all other shots on Torso 2, there was no indication of internal

TABLE 3—*Calculated impact velocities and observed tip separation.*

Torso Number	Shot	Impact Velocity (m/sec)	Tip Separation
1	A1	71.0	No
1	B1	72.5	No
1	C1	75.3	At impact
1	D1	72.2	At impact
1	E1	70.7	At impact
1	F1	71.0	No
1	G1	80.8	No
1	H1	85.3	At impact
1	J1	88.4	At impact
1	K1	89.9	At impact
1	L1	91.7	At impact
1	M1	93.9	At impact
1	N1	79.9	No
1	P1	87.5	At impact
1	Q1	84.4	No
1	R1	81.1	Prior to and at impact
1	S1	82.9	At impact
1	T1	81.7	At impact
1	U1	83.5	No
1	V1	76.8	At impact
1	W1	84.7	No
1	X1	78.0	At impact
1	Y1	78.0	Prior to impact
1	Z1	74.4	At impact
1	A2	75.6	No
1	B2	78.0	At impact
2	A1	80.5	At impact
2	B1	81.7	No
2	C1	71.0	At impact
2	D1	75.9	At impact
2	E1	79.6	No
2	F1	80.2	At impact
2	G1	80.8	No
2	H1	81.1	No
2	J1	81.7	At impact
2	K1	81.7	At impact
2	L1	77.4	At impact
2	M1	75.0	Prior to impact
2	N1	81.7	At impact
2	P1	83.8	At impact
2	Q1	91.4	Prior to impact
2	R1	96.0	At impact
2	S1	80.8	At impact

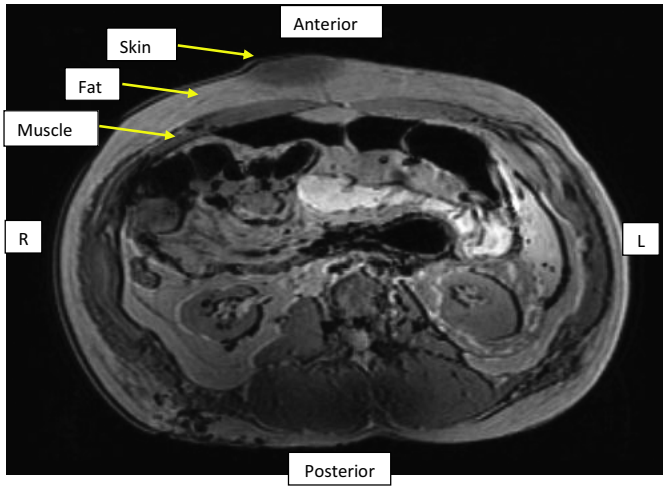

FIG. 3—*Representative posttest MR image of Torso 1 anterior impacts.*

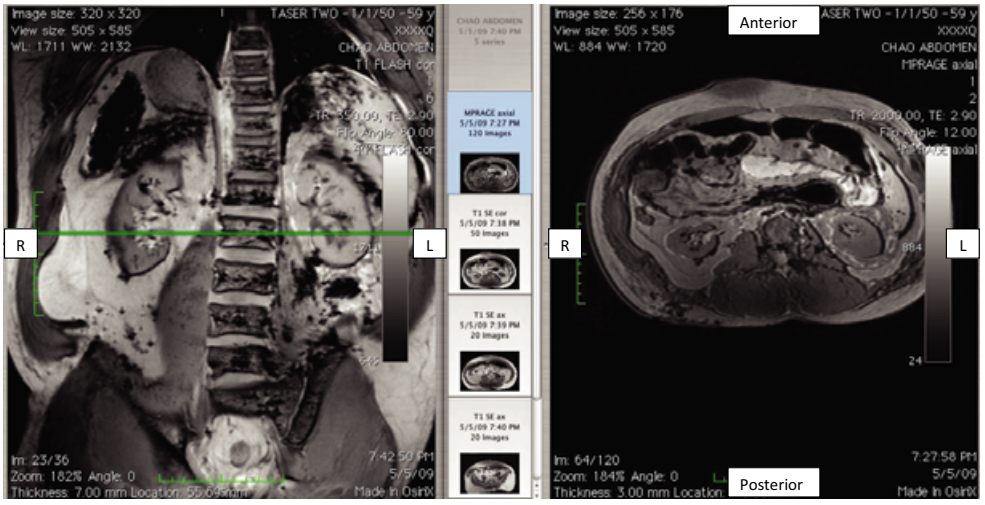

FIG. 4—*Representative posttest MR image of Torso 1 posterior impacts (shot 1L1). Left: coronal, right: axial.*

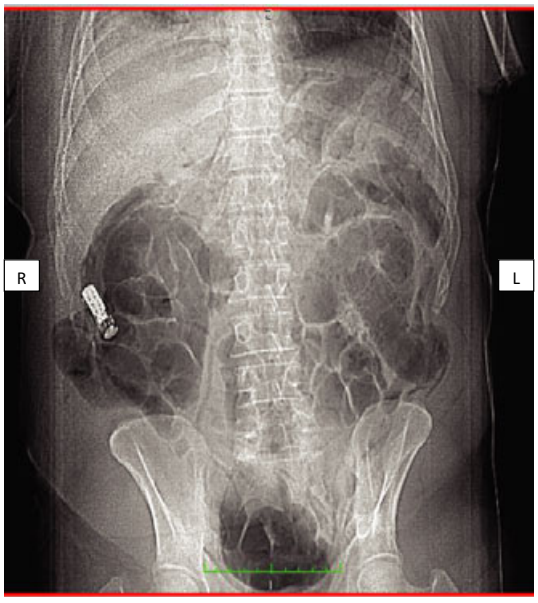

FIG. 5—*Posttest computed tomography image of Torso 2 with the shot 2Q1 extended range electronic projectile inside the abdomen (anterior view).*

damage in the vicinity of the XREP impacts or underlying the XREP impact sites that can be attributed to blunt impact trauma or penetration.

External inspection of Torso 1 showed evidence of surface impacts grouped in the following manner: on the anterior aspect, there were eight shots on the right side (torso as reference) (two on the thoracic region and six in the abdominal region) and five shots on the left side (one on the thoracic region and four in the abdominal region); and on the posterior aspect of the torso, there were four shots to the right side and three on the left; only two shots on the left (1M1 and 1L1) were located between rib number 12 and the iliac crest (in the retroperitoneal region).

Torso 1's abdominal wall thicknesses at three representative sections were *c.* 40 mm (with a fat layer of 20 mm). There was no evidence of punctures on the peritoneal surface of the anterior abdominal wall. The abdominal organs were removed so the retroperitoneal surface could be examined on the left side. The shots with the two highest impact velocities on the posterior aspect (1L1 and 1M1) were located externally at 120 mm from the left of midline and 20 and 60 mm inferior to the 12th rib, respectively. These locations were reproduced on the internal retroperitoneal surface, and no punctures were evident at these locations. The external locations of the three impacts (1Y1, 1N1, and 1X1) on the chest wall were then measured using the midline and sternal notch as reference points. The front of the chest wall was cut along the lateral margins through the ribs and reflected. The locations of the three points were reproduced on the internal pleural surface and no punctures were evident. With regard to the tests fired from 4.6 m (1A2 and 1B2), where the XREP achieved steady-state rotational velocity, there was no appreciable difference in penetration. The average thickness of skin to the pleural surface through the ribs was 40 mm.

External inspection of Torso 2 revealed only frontal impacts: in the abdominal region, seven on the right side (one shot penetrated the wall) and six to the left side; and in the thoracic region, three to the right side and one to the left side. Other than the one shot that breached the right side of the abdominal wall, there was no evidence of puncture of either the abdominal wall or the chest wall by the other shots. The average thickness of the abdominal and chest wall was 40–50 and 25–40 mm, respectively. This torso had previous surgery to the right lower quadrant, likely a hernia repair, as evident in the adherent tissue and an external scar. The shot that penetrated the abdomen (2Q1) went through the entire abdominal wall (Fig. 7) on the right side and was lodged in the mesentery without evidence of bowel perforation. It was not adherent to the retroperitoneal wall. The XREP was retrieved intact; however, the tip with the forward-projecting prongs was missing.

Discussion

The tested XREP impact velocities and corresponding injury evaluations are useful to determine the desired impact velocity in real-world applications. The latest XREP (7; release date: November 29, 2011) was designed to be fired either from a TASER X12TM by Mossberg® 12-gauge shotgun or any 18.5″ cylinder bore 12-gauge shotgun. When firing an XREP, the *muzzle* velocities for the X12 and other shotguns are *c.* 73.7 and 81.1 m/sec (7), respectively, which are on the lower end of the

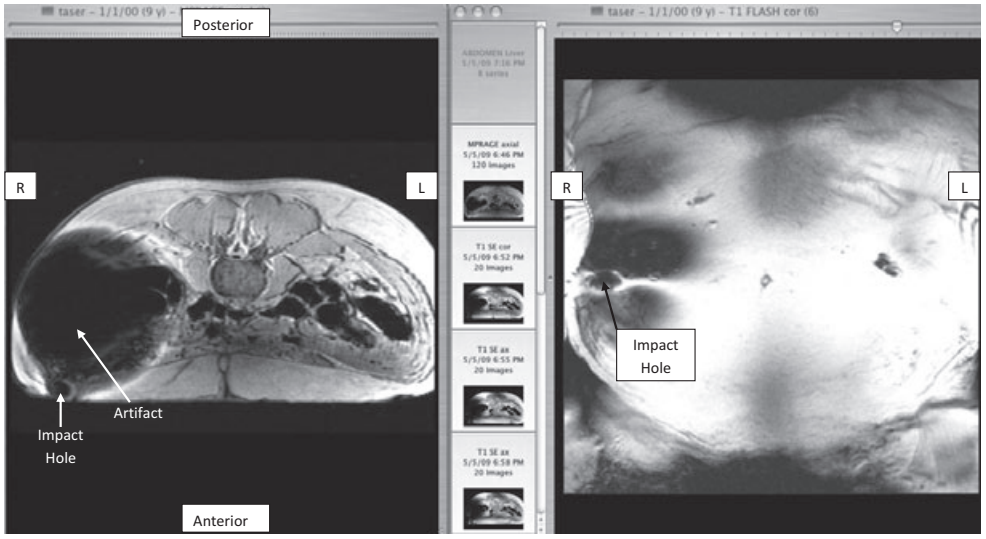

FIG. 6—*Posttest MR image of Torso 2 at the skin surface showing the penetration from shot 2Q1. Left: axial, Right: coronal.*

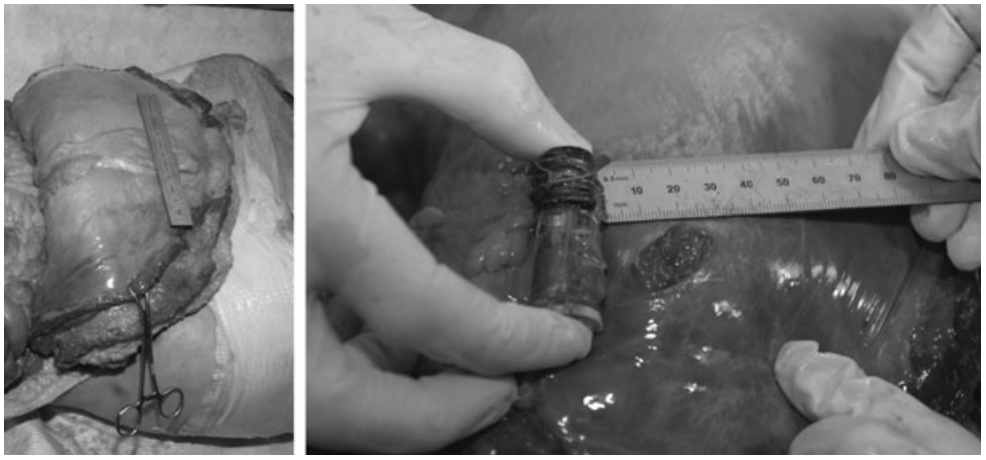

FIG. 7—*Left: Torso 1 abdominal wall reflected to examine peritoneal surface. Right: Torso 2 internal examination photograph of extended range electronic projectile penetration (shot 2Q1) showing damage to peritoneum.*

impact velocities observed in this study (70.6–95.9 m/sec). The specified range to fire the XREP is between 4.5 and 30.5 m (15 and 100 ft); thus, the corresponding *impact* velocities are less than those observed in this study. The air cannon was able to produce velocities greater than the real-world shotgun round, which is noteworthy considering the paucity of injuries observed in this test series.

The XREP premature tip separation was an artifact of the test equipment and has not been observed when fired from shotguns. The utilized air cannon was designed to fire the XREP by opening a high-speed valve once the desired compressed air pressure was achieved. The air entered the barrel and projected the XREP. The air cannon delivered greater amounts of compressed air than the actual design charge of the XREP. The geometry of the XREP is such that the diameter of the tip section is slightly larger than the body at its point of connection with the body (Fig. 2). In the tests that resulted in tip separation prior to impact with the torso, it is believed that the excess air caused the tip to separate from the XREP body. Regarding the one penetrating test (2Q1), if the tip did not separate prior to impact, it is less likely that penetration would have occurred.

Comparison to Injury Criteria

The VC was established based on animal testing performed at rates between 5 and 22 m/sec and on a series of cadaver testing performed at rates of 4.27 and 6.71 m/sec (1,8). Typical rates of ballistic testing are far beyond the range of validity of the VC. Thus, attempts to draw conclusions on injury outcomes from tests outside of this range of validity are speculative. Even within the rates of validity, certain loading mechanisms may result in less than positive correlations between the VC and injury outcomes. Kent et al. (9) performed seatbelt loading studies on cadaveric specimens at rates between 2.9 and 7.3 m/sec. They combined their data with other existing abdominal belt loading data and concluded that the VC was not the best predictor of injury outcomes and that the "relationship between compression and rate, particularly below 13 m/sec," is not robust.

Lau and Viano (1) defined a VC_{max} of 1.3 as a 50% risk of abbreviated injury scale (AIS) 4+ thoracic injury. As shown in Table 4, VC_{max} was larger than 1.3 m/sec in many of the XREP impacts. If VC_{max} was an appropriate measure of thoracic injury

for projectile impacts, the results obtained here would predict a greater than 50% risk of AIS 4+ injury for these impacts. Thoracic AIS 4+ injuries include flail chest, more than four rib fractures with hemothorax or pneumothorax, lung lacerations, aortic laceration, and major heart contusion. However, rib fractures, lung or aortic lacerations were not observed. We were unable to evaluate heart contusions. Therefore, VC_{max} = 1.3 m/sec is not likely a good predictor of injury outcomes in this regime and should be re-evaluated as an injury criterion at ballistic and blast rates.

TABLE 4—*Summary of VC_{max}, BC, and* E/A *for the XREP cadaver tests.*

Torso	Shot	XREP Mass at Impact (g)	Impact Velocity (m/sec)	VC_{max} (m/sec)	BC	*E/A* (J/cm^2)
1	A1	18.6	71.1	1.96	0.54	17.5
1	B1	18.6	72.4	0.11	0.58	18.1
1	C1	18.4	75.2	0.70	0.64	19.3
1	D1	18.6	72.3	0.55	0.58	18.1
1	E1	18.8	70.6	0.38	0.53	17.4
1	F1	18.5	71.1	0.27	0.54	17.4
1	G1	18.1	80.7	1.76	0.77	21.9
1	H1	18.0*	85.2	2.67	0.87	24.3
1	J1	18.3	88.4	2.39	0.96	26.6
1	K1	18.1	89.9	0.90	0.98	27.2
1	L1	18.0	91.8	1.96	1.02	28.1
1	M1	18.3	93.9	2.11	1.08	29.9
1	N1	18.2*	79.8	1.16	0.75	21.6
1	P1	18.5	87.6	0.63	0.95	26.4
1	Q1	18.5	84.6	1.07	0.88	24.6
1	R1	18.0*	81.0	2.59	0.77	22.0
1	S1	20.0	82.9	2.60	0.92	25.5
1	T1	18.6	81.8	0.43	0.82	23.1
1	U1	18.6	83.4	0.87	0.86	24.1
1	V1	18.2	76.8	0.91	0.67	20.0
1	W1	18.5	84.8	0.61	0.89	24.8
1	X1	18.9	78.1	0.23	0.74	21.4
1	Y1	19.5	78.2	2.33	0.78	22.1
1	Z1	18.5	74.4	0.89	0.63	19.0
1	A2	18.6	75.7	0.77	0.67	19.9
1	B2	18.5†	77.9	0.12	0.72	20.9
2	A1	18.5†	80.5	1.72	0.78	22.3
2	B1	18.5†	81.6	0.58	0.81	22.9
2	C1	18.4	71.2	1.63	0.53	17.4
2	D1	18.6	75.9	0.25	0.67	20.0
2	E1	18.1	79.5	0.96	0.74	21.3
2	F1	18.1	80.0	0.85	0.75	21.6
2	G1	18.4	80.7	0.63	0.78	22.3
2	H1	18.5	80.9	0.49	0.80	22.6
2	J1	18.4	81.6	0.22	0.80	22.8
2	K1	18.3	81.6	0.74	0.80	22.7
2	L1	18.4	77.4	0.37	0.70	20.5
2	M1	18.1	75.1	2.28	0.62	25.4
2	N1	18.5	81.8	0.81	0.81	23.0
2	P1	18.1*	83.8	1.03	0.84	23.6
2	Q1‡	18.1	91.5	4.65	1.02	37.7
2	R1	18.3	95.9	0.58	1.13	31.4
2	S1	18.5	80.8	0.32	0.79	22.4

BC, blunt criterion; *E/A,* energy density; VC, viscous criterion; XREP, extended range electronic projectile.

*The detachable tip of the XREP (see Fig. 2) was missing after the test. The mass reported was the sum of the mass of the body and the average of the masses of other tested XREP noses.

†The XREP was missing after the test series. The mass reported was the average of the other tested XREPs.

‡Impact 2Q1 penetrated the abdominal wall because of a combination of high impact velocity and reduced impact area. The recorded torso deformation was limited to the camera view and did not include the deformation within the torso.

A report by Clare et al. (2), from which the BC was derived, compiled various impact tests involving experimental impactors fired into the lateral thoraces and abdomens of dogs, goats, and pigs. The injury severity measure was either death or liver fracture. The majority of the tests were conducted using impactors with higher masses and speeds relative to the XREP; however, a subset of these data included tests using impactors and velocities (11.7 g, 80 m/sec, 27.6 mm diameter) comparable to the XREP design. Interestingly, the results of this subset indicated nonlethal impacts to the lateral thorax and absence of liver "fracture." The data from the tests investigating liver fracture vulnerability were averaged to calculate BC. In the Clare report, the goat torso thickness T (see Eq. [2]) was not provided for the nonlethal tests; thus, the average torso thickness from the lethal tests (2.49 cm^2) was used in the BC calculation. The corresponding BC average ± 1 standard deviation was 0.34 ± 0.64 (range: −1.34 to 2.18) for the tests that did not result in liver fracture and 1.14 ± 0.70 (range: −0.70 to 2.31) for the tests that resulted in liver fracture. The calculated BC values were significantly different based on a Student's t-test ($p < 0.01$). VC_{max} was not able to be calculated because data time histories were not provided in the Clare et al. (2) report. For comparison, the BC was calculated for the XREP cadaver tests. As shown in Table 4, the XREP BC average ± 1 standard deviation was 0.78 ± 0.15 (range: 0.51–1.13). As shown in the tabulated results, all of these were below the average BC calculated by Clare et al. (2) for liver fracture. Considering that the data in the Clare et al. (2) are from animal testing, the data are not directly comparable to the current test series; however, the corresponding BC results are noteworthy. Accounting for the BC results in the current test series, perhaps a higher BC than the average BC calculated from the Clare et al. (2) data are more appropriate as an injury criterion.

As shown in Eq. (2), BC is unique relative to the other criteria in this paper in that it includes torso geometry; a thinner layer of skin–muscle–fat at the impact location increases the risk of blunt injury. It is noteworthy that this study included two cadavers with the same body mass, nearly the same BMI, and as measured in autopsy nearly the same abdominal wall thickness. On face value, according to the BC, individuals with similar abdominal wall muscle thickness but less abdominal fat have increased risk of injury. However, the protective contribution of fat or muscle to the thickness aspect in the BC equation is unlikely to be equal; the resilience to penetration is obviously different between fat and muscle. The skin and muscle layers would not thin proportionately, and a thinner individual may be more muscular (i.e., larger torso thickness). Therefore, thinner individuals should not necessarily be perceived as having larger risk of penetration to the XREP.

The most comparable study to the present paper was performed by Bir and Viano (10). They conducted ballistic impacts on cadavers and calculated both VC_{max} and BC. Three test conditions were used as defined by the impactor mass and firing velocity: (i) 140 g, 20 m/sec; (ii) 140 g, 40 m/sec; and (iii) 30 g, 60 m/sec. The impactor was a 37-mm-diameter noncompressible baton and the target on the cadaver was center sternum. Based on a logistic regression of their results, they reported that a VC_{max} of 0.8 m/sec and a BC of 0.37 corresponded to a 50% chance of AIS 2 or 3 thoracic skeletal injury. Excluding the penetration test 2Q1, the XREP VC_{max} average ± 1 standard deviation was 1.14 ± 0.94 (range: 0.11–2.67). The average VC_{max} associated with the XREP is thus greater than the associated 50% risk value reported by Bir and Viano (10). As shown in Table 4, the XREP BC ranged between 0.51 and 1.13, suggesting

that based on Bir and Viano's (10) threshold there was a greater than 50% chance for AIS 2 or 3 thoracic skeletal injury for all of the XREP impacts. AIS 2 or 3 thoracic skeletal injuries include 2–3 rib fractures or sternal fracture, or more than four rib fractures unilaterally or 2–3 rib fractures with hemothorax or pneumothorax. In the XREP experiments, there was no evidence of blunt trauma from any of the impacts, which indicates that the Bir and Viano VC_{max} and BC 50% risk values (10) may be too low. It is noteworthy that in the Bir and Viano test series (10), the goal was to impact each specimen with each test condition. After each impact, the sternum was palpated to identify fracture. If fracture was identified, it was assumed that the fracture occurred during the last impact. This experimental technique could be misleading if microfracture occurred during the impact prior to the impact with identifiable fracture. Microfracture, which is not classified in the AIS, could decrease the integrity of the bone and thus decrease the VC_{max} and BC sufficient for injury. If the XREP data set were added to the Bir and Viano (10) data set, the probability function would be shifted to the right resulting in larger VC_{max} and BC values corresponding to a 50% chance of AIS 2 or 3 injury.

Sherman and Bir (11) performed impact tests on cadaver skulls using a 10.3-g, 38-mm-diameter rigid impactor fired at *c*. 20 m/sec. Of note, they reported that a 50% risk of skull fracture corresponded to a BC of 1.61.

Bir et al. (12) conducted a cadaveric study of skin penetration using 12-gauge, fin-stabilized rubber rockets. In that study, the rockets were fired into the abdomen, thorax, and legs of the cadavers at velocities ranging from 61 to 183 m/sec (200–600 ft/sec). The average mass and cross-sectional area of the rubber rocket was 6.40 g and 2.45 cm^2. From those tests, Bir et al. (12) calculated *E/A* for various regions on the thorax and developed corresponding risk functions. From the tests in the current paper, the XREP impact *E/A* was calculated to evaluate penetration potential and to compare to the Bir et al. 50% risk tolerance levels (12) (Table 5). The corresponding *E/A* ranged from 17.4 to 31.4 J/cm^2 for the nonpenetrating tests and 37.7 J/cm^2 for the penetrating test (2Q1). The higher *E/A* in the penetrating test was a result of both the high impact velocity (91.4 m/sec, 300 ft/sec) and small impact cross-sectional area because of the tip separation. For impacts on the anterior rib, the Bir et al. 50% risk *E/A* (12) was within 1 standard deviation of the XREP *E/A*. Because there were no penetrations in the anterior rib region in the XREP data set, this indicates that the Bir et al. 50% risk value (12) was likely too low. For the liver and lateral to umbilicus regions, the XREP *E/A* values were lower than the Bir et al. 50% risk values (12), which supported the 50% risk values for these regions. In addition, the penetrating test was in the lateral to umbilicus region, which also supported the 50% risk value for that region. For the posterior XREP impacts, the resulting *E/A* on the posterior ribs was 20.8 ± 4.18 J/cm^2 and the *E/A* in the posterior region between the 12th rib and the iliac crest was 29.4 ± 0.94 J/cm^2. It should be noted that in a data set without any penetrations, the data are entirely left censored, which means that the XREP *E/A* that is sufficient to cause XREP penetration is unknown; thus, an injury risk function cannot be generated with this data set alone.

TABLE 5—E/A *results for the exponent's nonpenetrating anterior XREP impacts compared to the Bir et al. 50% risk values (12).*

Location (n = Total Shots)	*E/A*, XREP Tests (J/cm^2)	*E/A*, Wayne State 50% Risk (J/cm^2)
On anterior rib (n = 8)	22.7 ± 1.92	23.99
Between anterior rib (n = 1)	31.4	33.30
Liver (n = 8)	21.2 ± 2.37	39.88
Lateral to umbilicus (n = 13)	23.7 ± 4.56	34.34

XREP, extended range electronic projectile.
There was only one test that impacted the area between the anterior ribs.

Interestingly, the velocities tested in this study (71–96 m/sec) are similar to those reported in earlier skin penetration studies from which velocity thresholds were derived for missiles and bullets. As discussed in the study by DiMaio (13), skin penetrations were found by others at *c*. 60–70 m/sec using projectiles smaller in diameter and of mass less than the TASER XREP. As shown in the *E/A* equation, both mass and cross-sectional area contribute to penetration risk and are inversely related. However, in this equation's denominator, the diameter is squared which has a greater effect on the *E/A* magnitude than mass, thus reducing the overall penetration potential. Further, this indicates that for a given impact velocity, a greater surface density (mass/area) increases the penetration risk. This may explain the lack of penetrations found in this study.

Limitations

There were several limitations in this investigation. The test surrogate was a cadaveric human torso, which obviously did not exhibit the physiology required to evaluate evolving trauma such as contusions. A test series using anesthetized animals could supplement the findings of the current study and address physiological vulnerabilities. Further, the use of MRI and CT in this study was indicated and designed to address the issues of structural anatomy and not physiological response to impact trauma. Although soft-tissue contrast in MRI is modified by temperature and decomposition, it can still be obtained with appropriate selection of pulse sequence timing parameters. CT contrast is also useful postmortem to demonstrate more subtle fractures than can be seen on MRI. It is acknowledged that bruising could be expected as a result of impact by the TASER device. Evaluation of this effect, which is considered relatively minor and highly unlikely to be life-threatening, was outside of the scope of the study.

The current sample size was small, which should be considered when identifying injury metrics such as BC or *E/A*. This sample size limitation is also present in other cadaveric ballistic studies and is an inherent limitation for cadaver studies in general. When interpreting the results from these studies, statistical significance and statistical power should be considered. In regard to establishing an appropriate injury criterion, a major limitation is the lack of injurious tests. With the exception of one test, the entire test series data set was left censored. To achieve injurious tests, the impact velocity could be increased and the resulting data could be added to the current data set. A survival analysis could be applied to the combined data set and an injury risk function could be generated.

The focus of this study was blunt impact to the torso region of the cadaver. Impacts to the face and extremities were not investigated. While the XREP projectile is reported to be accurate within the intended range of usage, the chance of inadvertent contact to the target's face or skull is still a possibility. Further research is necessary to evaluate the injury potential of facial contact. In addition, the XREP's neuromuscular effects were not evaluated in this study.

Conclusions

The TASER XREP was analyzed for blunt impact and penetration injury potential using cadaveric testing. Other than the one shot on Torso 2 (shot 2Q1—91.4 m/sec, 300 ft/sec) that penetrated the abdominal wall, there was no evidence of punctures through the abdominal, thoracic, or the retroperitoneal wall in both torsos from the any of the other shots. Further research is necessary to identify an appropriate injury criterion for both blunt and penetration trauma at the conditions tested in this study.

References

1. Lau IV, Viano DC. The viscous criterion—bases and applications of an injury severity index for soft tissues. Proceedings of the 30th STAPP Car Crash Conference; 1986 Oct 27–29; San Diego, CA. Ann Arbor, MI: The Stapp Association, 1986; SAE Paper No. 861882.
2. Clare VR, Mickiewicz AP, Lewis JH, Sturdivan LM. Blunt trauma data correlation. Aberdeen Proving Ground, MD: Edgewood Arsenal, 1975; Technical Report No. EB-TR-75106.
3. Sturdivan LM, Viano DC, Champion HR. Analysis of injury criteria to assess chest and abdominal injury risks in blunt and ballistic impacts. J Trauma 2004;56(3):651–63.
4. Chou CC, Lin YS, Lim GG. An evaluation of various viscous criterion computational algorithms. Proceedings from the SAE International Congress & Exposition; 1993 Mar 1–5; Detroit, MI. Warrendale, PA: SAE International, 1993; SAE Paper No. 930100.
5. Society of Automotive Engineers. Surface vehicle information report: injury calculations guidelines. Warrendale, PA: SAE International, 1996; Aug Report No.: SAE J1727.
6. Society of Automotive Engineers. Instrumentation for impact test—part 1—electronic instrumentation. Warrendale, PA: SAE International, 1995; Mar Report No.: SAE J211/1.
7. TASER International, Inc. TASER XREP electronic control device (ECD) specifications v. 4.0. Scottsdale, AZ: TASER International, Inc., 2011.
8. Viano DC, Lau IV. A viscous tolerance criterion for soft tissue injury assessment. J Biomech 1988;21(5):387–99.
9. Kent R, Stacey S, Kindig M, Woods W, Evans J, Rouhana SW, et al. Biomechanical response of the pediatric abdomen, part 2: injuries and their correlation with engineering parameters. Stapp Car Crash J 2008;52:1–32.
10. Bir C, Viano DC. Design and injury assessment criteria for blunt ballistic impacts. J Trauma 2004;57:1218–24.
11. Sherman D, Bir C. A test methodology for the complete characterization of the TASER XREP munition. Proceedings from the 5th European Symposium on Non-Lethal Weapons; 2009 May 11–13; Ettlingen, Germany. Pfinztal, Berghausen: Fraunhofer Institut Chemische Technologie, 2009.
12. Bir CA, Stewart SJ, Wilhelm M. Skin penetration assessment of less lethal kinetic energy munitions. J Forensic Sci 2005;50(6):1–4.
13. DiMaio VJ. Penetration and perforation of skin by bullets and missiles. Am J Forensic Med Pathol 1984;2(2):107–10.

Additional information and reprint requests:
Scott R. Lucas, Ph.D., P.E.
ECRI Institute
5200 Butler Pike
Plymouth Meeting, PA 19462
E-mail: slucas@ecri.org